

Copolymerization of the Silane-Modified Polyvinylimidazole(1) as a Metal Corrosion Inhibitor

JYONGSIK JANG* and HYUNCHEOL KIM

Department of Chemical Technology, Seoul National University, San 56-1, Shinlimdong Kwanakgu, Seoul, Korea

SYNOPSIS

The free radical copolymerization of vinyl imidazole (VI) with γ -methacryloxypropyltrimethoxy silane (γ -MPS) by using azobisisobutyronitrile (AIBN) as an initiator was carried out in benzene at 68°C. The copolymer compositions at various monomer feeds were investigated by elemental analysis. The reactivity ratios of two monomers were determined by the Finemann-Ross method: $r_1(\text{VI}) = 0.22$, $r_2(\gamma\text{-MPS}) = 3.18$. From these results, it could be concluded that silane-modified polyvinylimidazoles were random copolymers ($0 < r_1 r_2 < 1$). Thermal stability of the copolymer increased with increasing the mole ratio of VI in the copolymer. Thermal decomposition of the copolymer was caused by the decomposition of the γ -MPS unit. However, thermal stability above 300°C and maximum thermal decomposition temperature increased with increasing the mole ratio of γ -MPS due to the crosslinking reaction of hydrolyzed γ -MPS unit. © 1995 John Wiley & Sons, Inc.

INTRODUCTION

Protective organic coatings have been widely used as suppressing materials for metal corrosion during the service life. In the copper industry, new corrosion inhibitors have been constantly searched for various applications. In the case of printed circuit board manufacturing, it must be protected against copper corrosion after the etching process. After the copper surface was etched, it is exposed to the severe environments of a factory for a long time until it is coated with resistance ink. Therefore, organic coating of the copper surface with a corrosion inhibitor is necessary to protect the copper surface in a corrosive environment. However, the protecting layer, which is composed of small molecules (e.g., benzotriazole), is usually removed before printing resistance ink due to not only poor adhesion between resistance ink and the copper surface but also poor electrical and mechanical properties of this boundary region. Consequently, new polymeric agents have been investigated to prevent copper corrosion and that have good electrical and mechanical properties.

It has been reported that imidazole derivatives have high reactivity with copper surface, and that the complex formation between copper and nitrogen in the imidazole ring inhibits the diffusion of oxygen through the copper surface.¹⁻¹¹ Eng et al. reported that polyvinylimidazole (PVI) suppressed the oxidation of copper even at 400°C and had better film properties of ductility, uniformity, and chemical resistance than small molecules.¹²⁻¹⁴

However, PVI and other imidazoles cannot inhibit the corrosion of the copper surface in humid condition. Therefore, a silane-coupling agent was introduced to overcome this weakness of PVI and improve the adhesion between polymer film and copper. Silane-coupling agent has the structure of $X_3\text{SiY}$, and X is composed of chlorine or alkoxy and Y represents organic functional group. The hydrolysis of silane coupling agent provides the Si—OH from the alkoxy group, which can react with the inorganic surface. In the case of vinyl silane derivatives, the copolymerization of silane-coupling agent and VI forms the silane modified PVI(1). The role of silane-coupling agent in the copolymer is that it forms chemical bonding with copper surface to improve the adhesion between copper and coated copolymer and to

* To whom correspondence should be addressed.

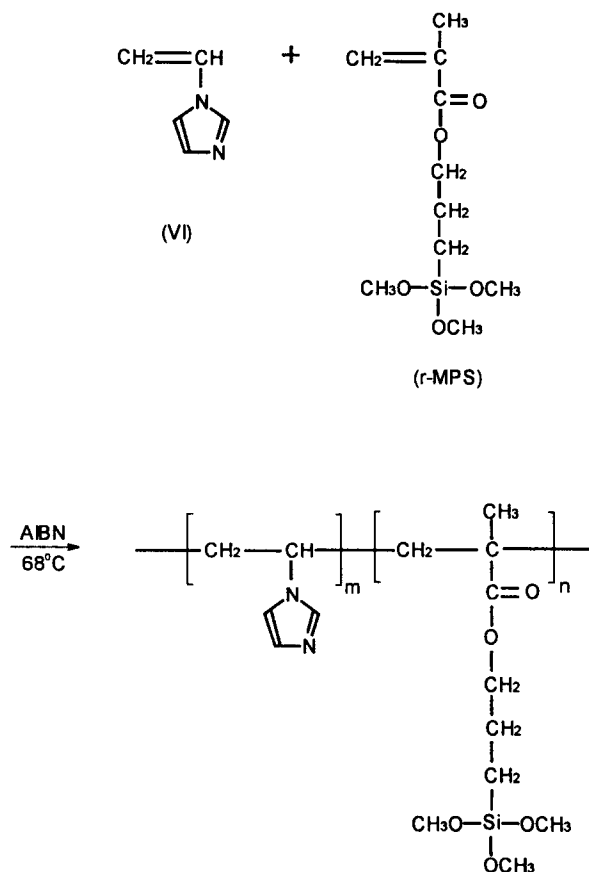


Figure 1 The copolymerization scheme of VI and γ -MPS.

exclude water molecule at the metal-polymer interface.¹⁵⁻¹⁸

Jang et al. reported that silane-modified PVI could suppress the corrosion of copper in humid conditions and an elevated temperature environment.¹⁹ The corrosion process on the copolymer-coated copper depends on the treating time at elevated temperature but not strongly on the coated film thickness. At a high content of γ -methacryloxypropyltrimethoxy (γ -MPS), thermal degradation

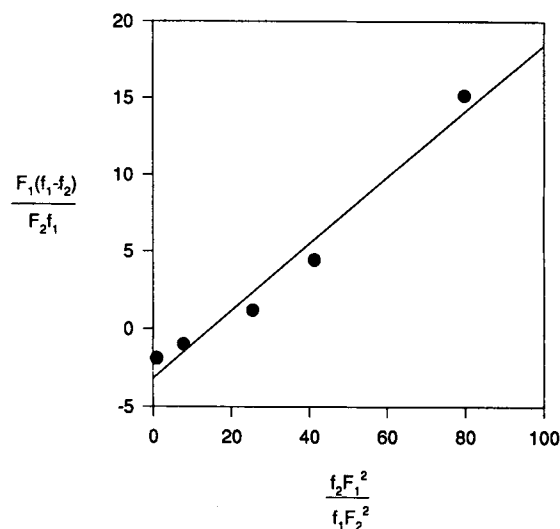


Figure 2 Finemann-Ross plot for the determination of reactivity ratio.

of silane-coupling agent might mainly affect the corrosion formation of the copper surface. Adhesion tests indicated that silane-modified PVI had much better adhesion property than PVI.

In this study, the copolymer compositions at various monomer feeds were investigated by thermal analysis and elemental analysis, and the relative reactivities of two feed monomers were determined by the Finemann-Ross method. It is the purpose of this work, therefore, to understand the role of silane-coupling agents in the corrosion inhibition on copper and study the thermal stability of silane-modified PVI(1) for the copper corrosion protection.

EXPERIMENTAL

Vinyl imidazole (VI) was purchased from Aldrich Chemical Co. and distilled in vacuum (80°C/1 mmHg) to yield a pure and colorless liquid. γ -MPS was purchased from Petrach Systems Inc. and also

Table I Data for the Elemental Analysis and the Copolymer Compositions

Feed Ratio (VI : γ -MPS)	C (wt %)	H (wt %)	N (wt %)	VI (mol %)	γ -MPS (mol %)	Conversion (%)
1 (95 : 5)	55.12	7.53	19.72	83.20	16.80	6.8
2 (90 : 10)	50.41	7.45	12.73	66.20	33.80	8.3
3 (85 : 15)	49.38	7.62	9.52	55.74	44.26	8.7
4 (70 : 30)	42.80	6.85	6.29	41.33	58.67	8.0
5 (30 : 70)	46.36	7.90	2.00	15.50	84.50	9.2

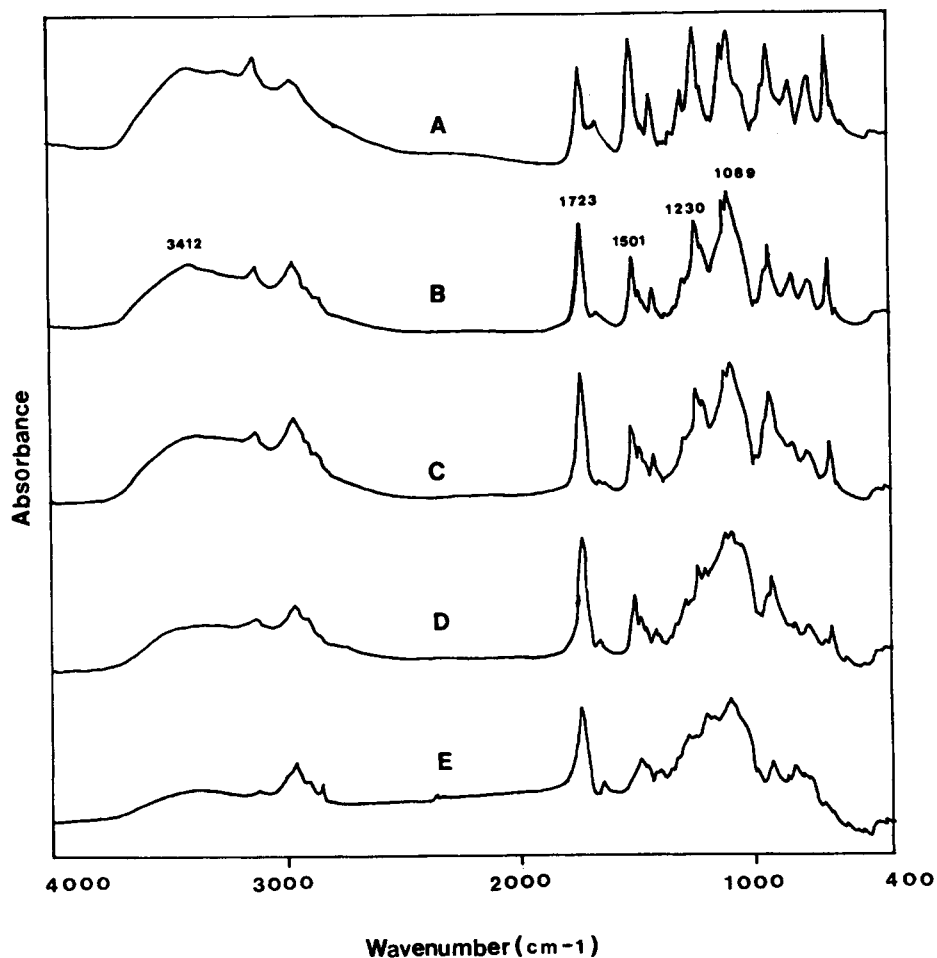


Figure 3 FT-IR transmission spectra of the copolymers with different mole ratios (VI/ γ -MPS). (A) 95/5, (B) 90/10, (C) 85/15, (D) 70/30, and (E) 30/70.

distilled in vacuum (80°C/13 mmHg) for this study. Azobisisobutyronitrile (AIBN) from Wako Pure Chemical Industries, Ltd. was dissolved in warm methanol (35°C), recrystallized in an ice bath, and then dried in a vacuum oven at room temperature for two days.

Silane-modified PVI(1)s were synthesized by free radical copolymerization using AIBN as an initiator. VI and γ -MPS were polymerized in benzene at 68°C with stirring in nitrogen atmosphere for 24 h. The total monomer concentration was 2M, and the initiator concentration was fixed at 2×10^{-3} M. The copolymerization scheme of VI and γ -MPS is represented in Figure 1.

After the period required (45–90 min) for copolymerization, the contents were pipetted, immediately cooled, and precipitated by a large volume of *n*-hexane. The precipitated polymers were collected by filtration, washed with benzene, and

finally dried in a vacuum oven at room temperature for 2 days.

For the study of thermal stability of copolymers with different mole ratios of γ -MPS, complete copolymer was synthesized in the same condition.

The hydrolysis of copolymer (VI/ γ -MPS = 90/10) was carried out under the different pH condition. After mixed solvent of isopropyl alcohol-water was used to dissolve the precipitated copolymer, the solution pH was controlled by adding acetic acid. Hydrolysis time of copolymer was fixed at 1 h.

The composition of copolymers was determined by carbon, hydrogen, and nitrogen analysis using YANACO MT-2 elemental analyzer. The column temperature was maintained at 850°C during the combustion and at 550°C during the reduction. He and O₂ were used as carrier gases and the detector temperature was 55°C.

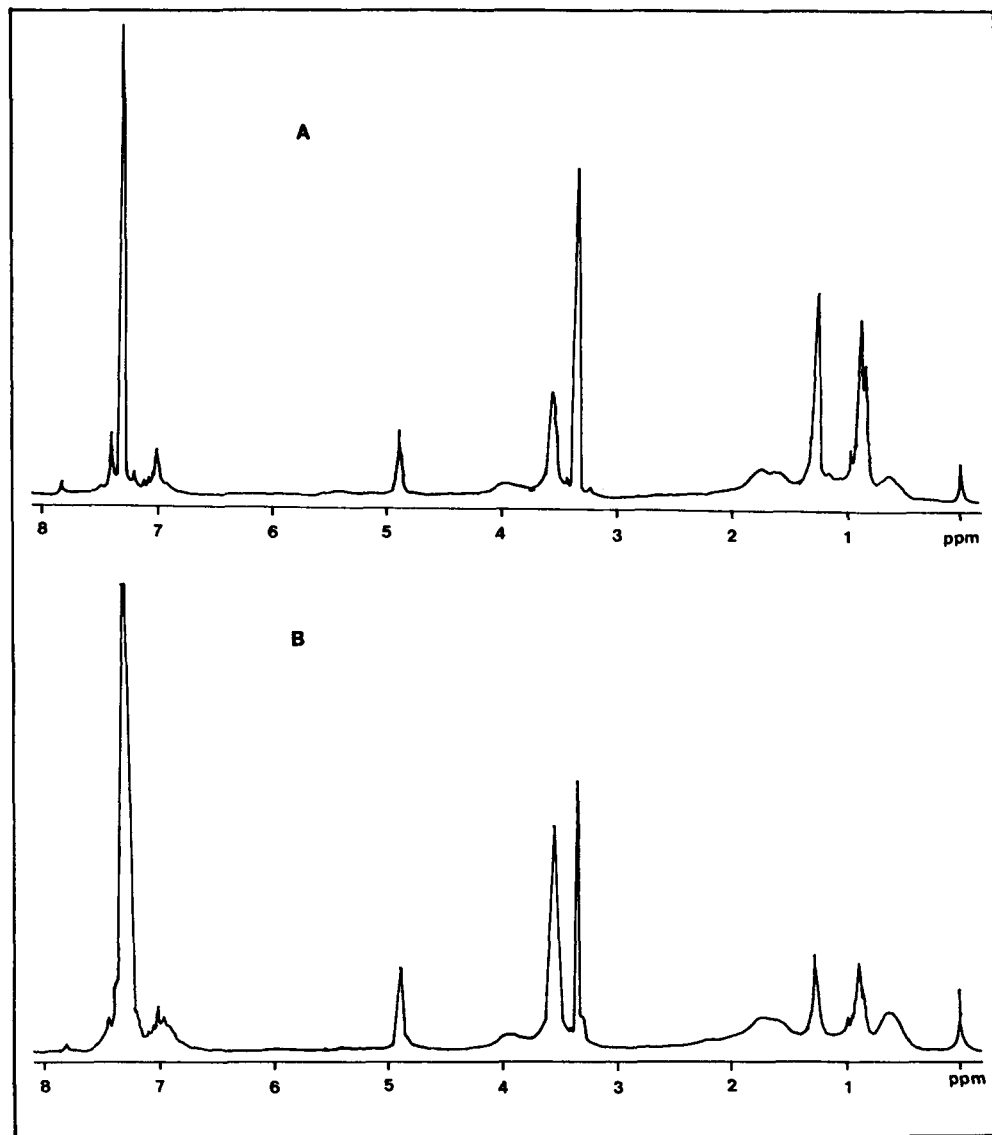


Figure 4 $^1\text{H-NMR}$ spectra of the copolymers dissolved in CD_3OD . (A) VI/ γ -MPS = 70/30 and (B) VI/ γ -MPS = 85/15.

Copolymers were characterized using Perkin-Elmer 1725-X Fourier transform infrared (FT-IR) spectrophotometer by KBr tablet method. Spectrum analysis was performed with the average of 64 scans at 2 cm^{-1} resolution.

The $^1\text{H-NMR}$ spectra of copolymers dissolved in CD_3OD was obtained by using VXR-200 FT-NMR spectrophotometer. Tetramethyl silane was used as an internal standard material.

Thermal behaviors of copolymers were investigated by using a Perkin-Elmer TGA7 thermogravimetric analyzer at a heating rate of $10^\circ\text{C}/\text{min}$ in N_2 atmosphere, and Perkin-Elmer DSC7 differential

scanning calorimetry at a heating rate of $20^\circ\text{C}/\text{min}$ in the N_2 atmosphere.

RESULTS AND DISCUSSION

Determination of reactivity ratios

The copolymer compositions can be determined by elemental analysis. The data for the elemental analysis and the copolymer compositions are given in Table I. It shows that the mole fraction of γ -MPS in the copolymer is higher than that in the feed. The

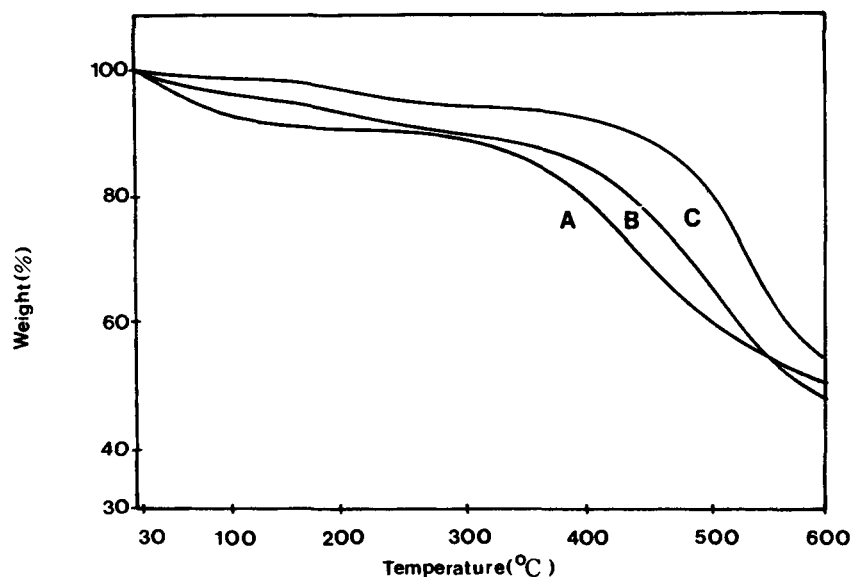


Figure 5 TGA trace of the copolymers with different mole ratios (VI : γ -MPS) in nitrogen atmosphere. (A) 95/5, (B) 70/30, and (C) 30/70.

copolymer conversions were kept below 10%, and the copolymer compositions could be determined on the basis of nitrogen contents in the elemental analysis data.

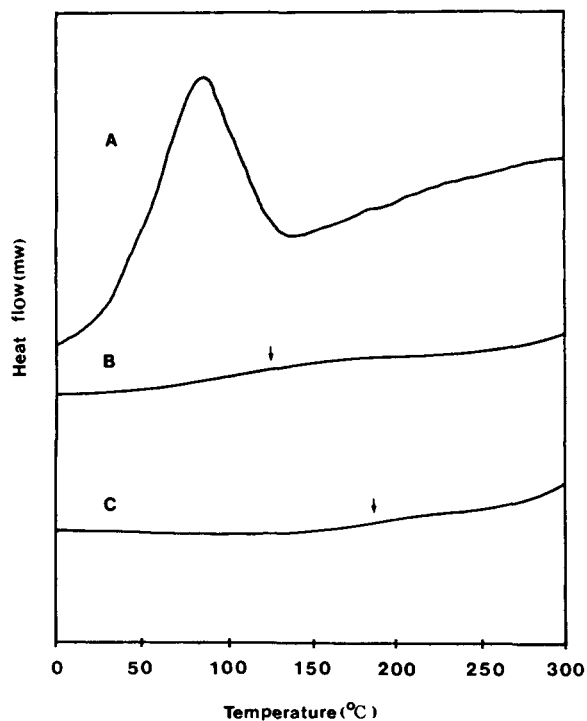


Figure 6 DSC curves of PVI and the copolymer (VI : γ -MPS = 30 : 70). (A) PVI, (B) the first scan of the copolymer, and (C) the second scan of the copolymer.

The reactivity ratios were determined by the Finemann–Ross method, which is widely used in low conversion. The copolymer composition is given by the equation of Mayo and Lewis as²⁰

$$\frac{f_1}{f_2} = \frac{r_1 F_1^2 + F_1 F_2}{r_2 F_2^2 + F_1 F_2}$$

where F_1 and F_2 are the mole fractions of the two monomers 1 and 2 in the feed, and f_1 and f_2 are the mole fractions in the copolymer. Finemann and Ross rearranged this equation as

$$\frac{F_1 f_1 - f_2}{F_2 f_1} = \frac{f_2 F_1^2}{f_1 F_2} r_1 - r_2$$

A plot of $F_1(f_1 - f_2/F_2f_1)$ of the above equation versus $f_2F_1^2/f_1F_2$ gives a straight line with a slope. From this figure, r_1 is determined by the slope and r_2 is obtained by the intercept. The least-square Finemann–Ross plot is shown in Figure 2. From the figure, determined monomer reactivity ratios are $r_1(\text{VI}) = 0.22$, $r_2(\gamma\text{-MPS}) = 3.18$. These results for reactivity ratios of two monomers in the copolymerization process is explained by two factors: polarity of double bond and stabilization of radical.^{21,22} From the viewpoint of the former, both γ -MPS and VI have the poor π -electron density due to their electron withdrawing substituent. However, γ -MPS has the more polar double bond by the inductive effect of the methyl group and the higher monomer reactivity. Besides,

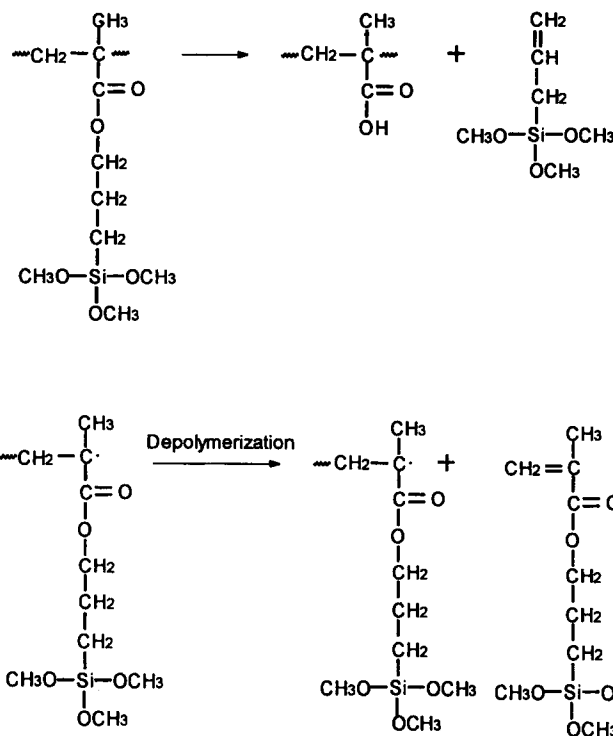


Figure 7 Thermal decomposition mechanism of the copolymer.

the γ -MPS radical has an increased stability through the hyperconjugation with the methyl group. Consequently, γ -MPS enters preferentially into polymer chain.

An examination of the reactivity ratios reveals that $r_1 r_2$ is 0.70, and that γ -MPS undergoes a random copolymerization with VI. Judging from the data $r_1(\text{VI}) < 1$ and $r_2(\gamma\text{-MPS}) > 1$, γ -MPS prefers homopropagation to cross-propagation and VI cross-propagation to homopropagation. Consequently, in the initial stage of reaction, γ -MPS mainly exists

in the copolymer, but the mole ratio of VI in the copolymer increases with reaction time because the feed ratio of VI increases as the reaction proceeds.

In the initial stage of the reaction, homopolymer of γ -MPS can appear due to the large difference of the two reactivity ratios. Homopolymer of γ -MPS in the polymer mixture is increased with increasing the feed ratio of γ -MPS. In the later stage of the reaction, homopolymer of VI can exist in the polymer mixture and its amount increases with increasing the feed ratio of VI.

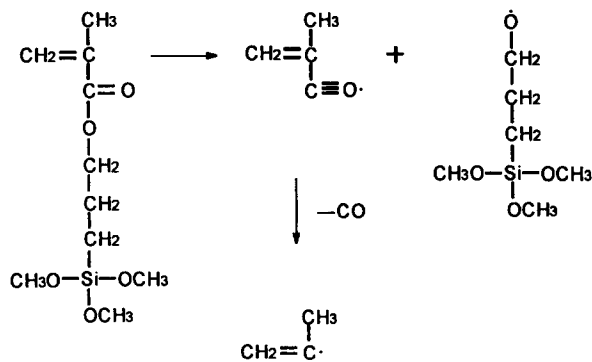


Figure 8 Thermal decomposition mechanism of γ -MPS.

Characterization of Copolymer

Figure 3 demonstrates the different transmission spectra of the copolymers as a function of the mole fraction. The band around 3412 cm^{-1} is assigned to the O—H stretching mode due to the water overtone. Solution polymerization in benzene causes PVI to have one-third mole of bound water per mole of monomer.¹³ However, synthesized copolymers have reduced the amount of bound water, especially at lower mole fraction of VI. The broad feature in the $3700\text{--}2800\text{ cm}^{-1}$ region is due to the hydrogen bonding with the residual bound water. The peak at 3116 cm^{-1} originates from the $\text{C}=\text{C}-\text{H}/\text{N}=\text{C}-\text{H}$

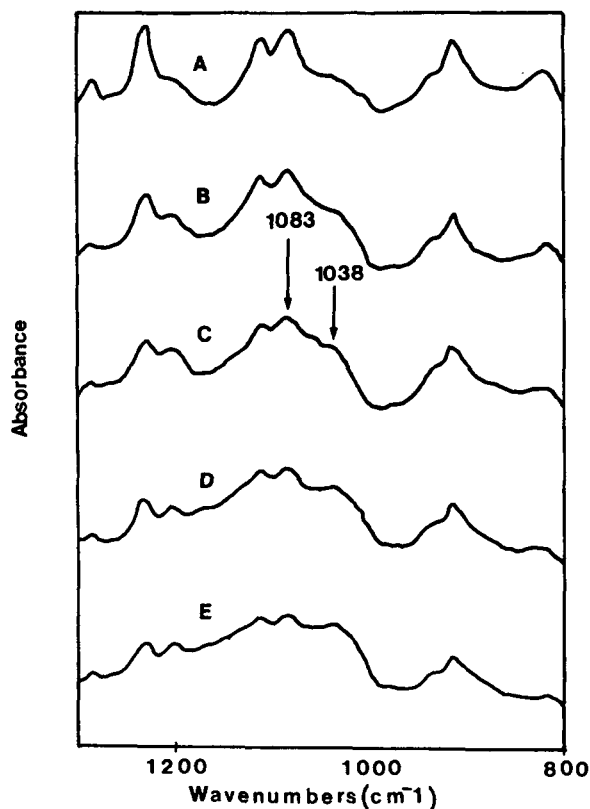


Figure 9 FT-IR transmission spectra from 1300 to 800 cm^{-1} of the copolymers modified PVI with different mole ratios (VI/ γ -MPS). (A) 95/5, (B) 90/10, (C) 85/15, (D) 70/30, and (E) 30/70.

stretching and the peak at 1501 cm^{-1} is due to the $\text{C}=\text{C}/\text{C}=\text{N}$ stretching. The free carbonyl peak appears at 1723 cm^{-1} and the peak at 1285 cm^{-1} is associated with the ester functionality of silane-coupling agent. The peak at 1230 cm^{-1} shows the ring vibration and the peak at 1089 cm^{-1} is designated to the $\text{Si}-\text{O}-\text{CH}_3$ bending. As the feed ratio of γ -MPS was increased, the characteristic peaks of γ -MPS at 1723 and 1089 cm^{-1} were increased in relative intensity, and those of VI at 3412 , 1500 , and 1230 cm^{-1} were decreased in relative intensity.

Figure 4 shows $^1\text{H-NMR}$ spectra of the copolymers dissolved in CD_3OD . As the feed ratio of γ -MPS was increased, the characteristic peaks of γ -MPS at $\delta = 0.6$, $\delta = 1.3$, $\delta = 1.7$, and $\delta = 3.6$ were increased in relative intensity, and those of VI between $\delta = 7$ and $\delta = 8$ decreased in intensity.

Thermal Analysis

Figure 5 shows the weight loss in the copolymers with increasing the temperature of the N_2 atmo-

sphere. The initial weight loss below 140°C is mainly due to the vaporization of residual water around the imidazole ring. As the mole ratio of VI of the copolymer was increased, initial weight loss was increased, and the copolymer, whose mole ratio of VI to γ -MPS is 30 : 70, showed only a little weight loss by water vaporization. The above fact has a good agreement with the differential scanning calorimetry (DSC) thermogram showing an exotherm peak at the interval of 20 to 140°C in Figure 6 (A). Maximum peak at 100°C indicates the exothermal peak due to the water vaporization. Figure 6 (B, C) shows the change in glass transition temperature (T_g) in DSC curves of the copolymer (VI : γ -MPS = 30 : 70). T_g in the second scan is higher than T_g in the first scan.

The weight loss of copolymer at the interval of 140 – 300°C in Figure 5 was increased with increasing the mole ratio of γ -MPS in the copolymer. It is thought to be caused by the thermal decomposition of the γ -MPS unit of the copolymer.²³ Generally, a polymer with a long side chain has a low ceiling temperature and easily tends to depolymerize because of radical formation on the main chain due to thermal decomposition. γ -MPS monomer formed by depolymerization produces volatile small molecules through a successive thermal decomposition. Eventually this small molecule brings about the weight loss of the copolymer. Besides, the ester bond in the γ -MPS unit of the copolymer easily can be thermally decomposed.

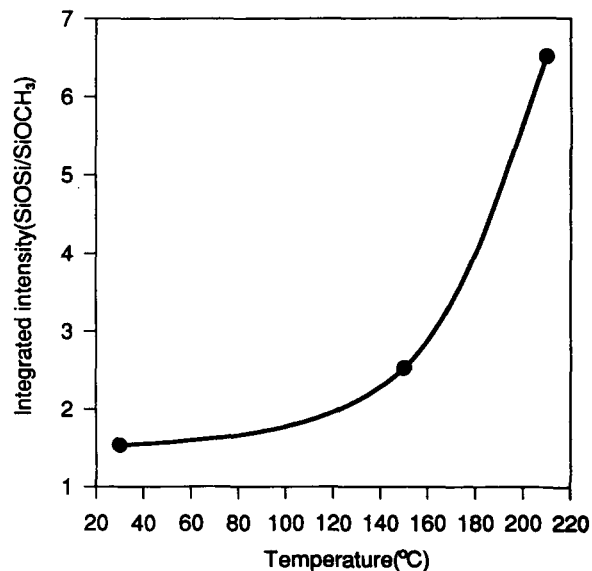


Figure 10 Integrated intensity ($\text{Si}-\text{O}-\text{Si}/\text{Si}-\text{O}-\text{C}$) of the copolymer (VI : γ -MPS = 70 : 30) as a function of temperature.

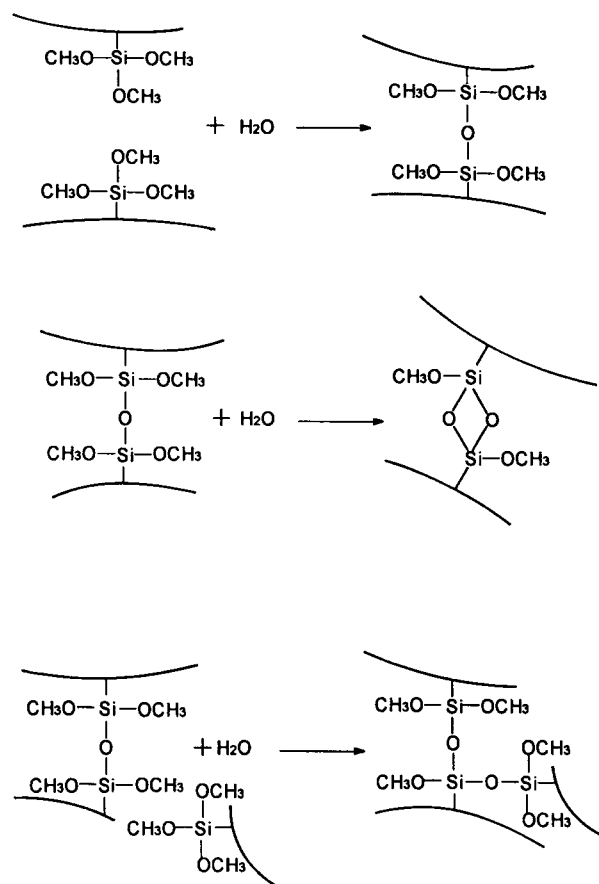


Figure 11 Crosslinking reactions of the copolymer.

Figure 7 shows the first thermal decomposition mechanism of the copolymer. It proceeds by the ester bond decomposition of the side chain and the depolymerization of the copolymer.

Figure 8 shows that γ -MPS monomer produced from first decomposition makes small fragments through the secondary thermal decomposition. C—O and C—C bonds in γ -MPS unit are easily decomposed by heat to form radical of small fragments and gas (e.g., CO). These small fragments of copolymer easily vaporize at high temperature and accelerate weight loss.

However, the temperature showing the maximum weight loss in Figure 5 increased with increasing γ -MPS content in the copolymer. This phenomenon can be explained by the crosslinking reaction of hydrolyzed γ -MPS in the copolymer. Figure 9 demonstrates the changes occurring in the transmission spectra from 1300 to 800 cm^{-1} of the copolymers as a function of mole fraction. As the feed ratio of γ -MPS increases, the characteristic peak of Si—O—C at 1088 cm^{-1} decreases in relative ab-

sorbance, and those of Si—O—Si at 1038 cm^{-1} increase in relative absorbance. This tendency indicates that crosslinking reaction by water increased with increasing γ -MPS content in the copolymer. The other crosslinking reaction is attributed to crosslinking by vaporized residual water during heating.^{24–28} It can be explained by Figure 6 (B, C) and Figure 10. In Figure 6 (B, C), higher T_g in the second scan suggests that crosslinking reaction by vaporized water occurred during heating. Figure 10 shows integrated intensity (Si—O—Si/Si—O—C) of mole fraction of copolymer (VI : γ -MPS = 7 : 3) as a function of temperature. Integrated intensity of copolymer increases gradually with increasing temperature, but increases drastically at the range of 150–200°C. Initial increase of integrated intensity is due to crosslinking reaction with residual water vaporized by heating, and drastic increase of integrated intensity is attributed to not only an increase in the Si—O—Si bond by crosslinking reaction but also a decrease in the Si—O—C bond by thermal decomposition. Decrease in Si—O—C bond is supported by weight loss at the range of 150–300°C in Figure 5 (B). These facts suggest that copolymer should undergo crosslinking reaction by vaporized residual water during heating.

Figure 11 shows a variety of crosslinking reaction processes in the copolymer. The γ -MPS units in the copolymer undergoes crosslinking reaction by water in air or vaporized residual water.

Hydrolysis of Copolymer

Figure 12 demonstrates FT-IR transmission spectra from 1100–900 cm^{-1} of the hydrolyzed copolymers at different pH. The characteristic peak of Si—O—C at 1088 cm^{-1} exists before hydrolysis, but this peak disappears after hydrolysis. This phenomenon indicates that Si—O—CH₃ is completely converted to Si—OH by hydrolysis. The peak at 1038 cm^{-1} after hydrolysis is assigned to the characteristic peak of the Si—O—Si bond formed by condensation reaction of Si—OH. As the solution pH is lowered, the characteristic peak of Si—O—Si at 1038 cm^{-1} is decreased in relative intensity and not observed at pH = 2.5. Consequently, the stability of silanol formed by hydrolysis is strongly affected by solution pH.

CONCLUSIONS

The copolymer of γ -MPS and VI, as a corrosion inhibitor, was synthesized using free radical copolymer-

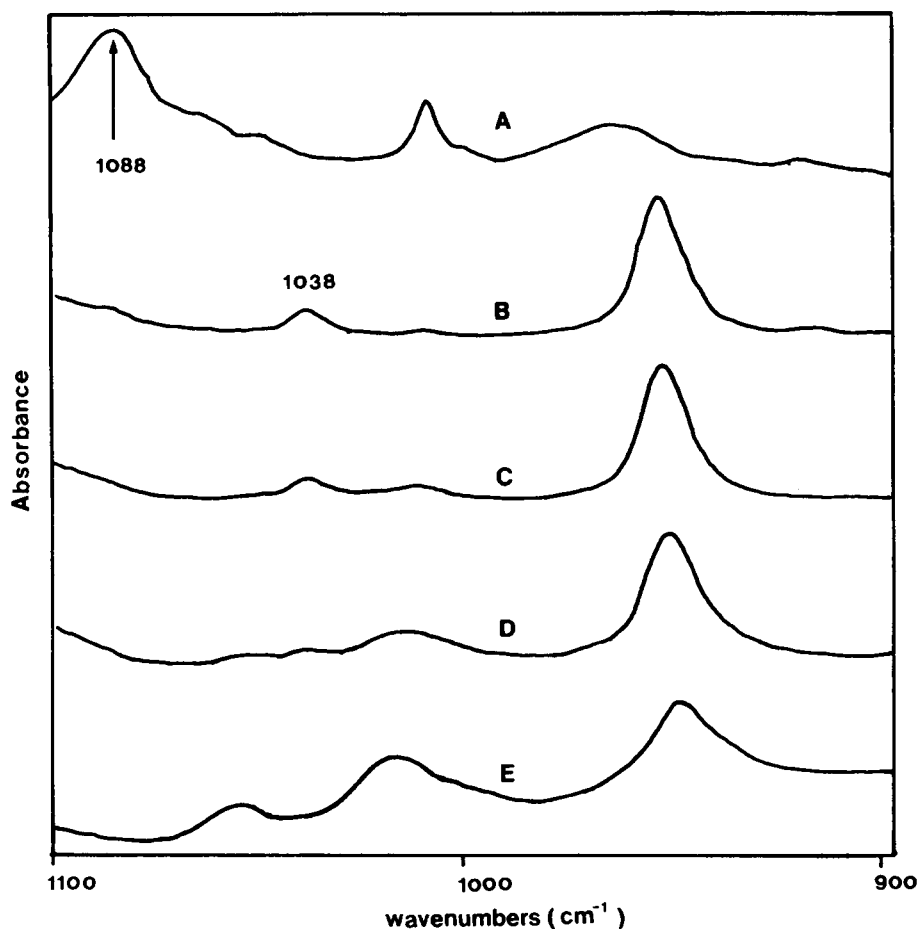


Figure 12 FT-IR transmission spectra of the hydrolyzed copolymer with different pHs. (A) Before hydrolysis, (B) pH = 7, (C) pH = 5.0, (D) pH = 3.5, and (E) pH = 2.5.

ization, and the reactivity ratios of two monomers are $r_1(\text{VI}) = 0.22$, $r_2(\gamma\text{-MPS}) = 3.18$. During the polymerization of copolymer, $\gamma\text{-MPS}$ prefers homopropagation to cross-propagation and VI cross-propagation to homopropagation. The synthesized copolymer is a random one ($0 < r_1 r_2 < 1$), which means the intermediate between alternating polymer and ideal polymer.

Thermal stability of copolymer below 300°C in the N_2 atmosphere increased with decreasing the mole ratio of $\gamma\text{-MPS}$ and maximum thermal decomposition temperature and vice versa. Weight loss of copolymer below 300°C is attributed to the thermal decomposition of the $\gamma\text{-MPS}$ unit, and thermal stability above 300°C is mainly due to the crosslinking reaction.

REFERENCES

1. J. Bauman and J. Wang, *Inorg. Chem.*, **3**, 368 (1964).
2. B. Chriswell, F. Lions, and B. Morris, *Inorg. Chem.*, **3**, 110 (1964).
3. M. Goodgame and Haines, *J. Chem. Soc. (A)*, **66**, 174 (1966).
4. W. Eilbeck, F. Holmes, and A. Underhill, *J. Chem. Soc. (A)*, **67**, 757 (1967).
5. W. Eilbeck, F. Holmes, C. Taylor, and A. Underhill, *J. Chem. Soc. (A)*, **68**, 128 (1968).
6. C. Taylor and A. Underhill, *J. Chem. Soc. (A)*, **69**, 368 (1969).
7. D. Doonan and A. Balch, *J. Am. Chem. Soc.*, **97**, 1404 (1975).
8. S. Salama and T. Spiro, *J. Am. Chem. Soc.*, **100**, 1105 (1978).
9. M. Mohan, D. Bancroft, and E. Abbett, *Inorg. Chem.*, **18**, 1527 (1979).
10. G. Kolks, C. Frikart, P. Coughlin, and S. Lippard, *Inorg. Chem.*, **20**, 2433 (1981).
11. L. Antolini, L. Battaglia, A. Carradi, G. Marcotrigiano, L. menabue, G. Pellacani, and M. Saladini, *Inorg. Chem.*, **21**, 1391 (1982).
12. F. Eng and H. Ishida, *J. Mat. Sci.*, **21**, 1561 (1986).
13. F. Eng and H. Ishida, *J. Appl. Polym. Sci.*, **32**, 5021 (1986).

14. F. Eng and H. Ishida, *J. Appl. Polym. Sci.*, **32**, 5035 (1986).
15. H. Ishida and K. Kelly, *Polymer*, **32**, 1585 (1991).
16. Edwin P. Plueddemann, *Silane Coupling Agents*, Plenum Press, New York, 1982.
17. S. Yoshida and H. Ishida, *J. Chem. Phys.*, **78**, 6960 (1983).
18. S. Yoshida and H. Ishida, *J. Mat. Sci.*, **19**, 2323 (1984).
19. J. Jang and H. Ishida, *J. Appl. Polym. Sci.*, **49**, 1957 (1993).
20. M. Fineman and S. D. Ross, *J. Polym. Sci.*, **2**, 259 (1950).
21. C. P. Reghunadhan Nair, G. Clouet, and J. Brossas, *J. Polym. Sci.: Part A: Polym. Chem.*, **26**, 1791 (1988).
22. Zbigniew Florjanczyk, Włodzimierz Krawiec, and Katarzyna Such, *J. Polym. Sci.: Part A: Polym. Chem.*, **28**, 795 (1990).
23. Indra K. Varma, Anil K., and R. C. Anand, *J. Appl. Polym. Sci.*, **33**, 1377 (1987).
24. T. Hjertberg, M. Palmlof, and B. A. Sultan, *J. Appl. Polym. Sci.*, **42**, 1185 (1991).
25. T. Hjertberg, M. Palmlof, and B. A. Sultan, *J. Appl. Polym. Sci.*, **42**, 1193 (1991).
26. Z. Florjanczyk and W. Krawiec, *Macromol. Chem.*, **190**, 2144 (1989).

Received July 6, 1994

Accepted January 8, 1995